Geophys. J. Int. (2003) **153,** 263–276

Palaeointensity study of the Hawaiian 1960 lava: implications for possible causes of erroneously high intensities

Y. Yamamoto,[1] H. Tsunakawa[2] and H. Shibuya[3]

[1] *Institute for Marine Resources and Environment, Geological Survey of Japan, AIST, Tsukuba* 305-8567, *Japan. E-mail: yuhji-yamamoto@aist.go.jp*
[2] *Department of Earth and Planetary Sciences, Tokyo Institute of Technology, Tokyo* 152-8551, *Japan*
[3] *Department of Earth Science, Kumamoto University, Kumamoto* 860-8555, *Japan*

Accepted 2002 November 5. Received 2002 October 30; in original form 2002 June 5

SUMMARY

It is known that the Hawaiian 1960 lava sometimes yields higher palaeointensities than the IGRF (36.2 μT). In order to clarify the causes, we have performed a comprehensive investigation of palaeointensity measurements on 19 cores from the lava. According to various rock magnetic analyses, they are classified into three groups with degrees of the deuteric oxidation. In Coe's version of the Thellier method, a significantly larger mean palaeointensity of 49.0 ± 9.6 μT ($N = 17$) was observed similar to previous studies. These palaeointensities showed a dependence on the oxidation indices, which can be explained by thermochemical remanent magnetization (TCRM) acquisition during the natural cooling stage of the lava. Although it is generally difficult to distinguish the TCRM from thermoremanent magnetization (TRM), a low-temperature demagnetization (LTD) treatment on NRM and TRM in the Thellier experiment seems to allow us to detect the influence of the TCRM on NRM. Another possible tool for TCRM detection is the double-heating technique (DHT) of the Shaw method combined with LTD (LTD–DHT Shaw method). It gave a better average of 39.4 ± 7.9 μT ($N = 9$), though the success rate was much lower. Most of the inappropriate results were screened by a combination of the double-heating test, the ARM correction and the LTD treatment. If two outliers are further excluded, the average is improved to be 35.7 ± 3.3 μT ($N = 7$), which agrees well with the expected intensity. The results of both methods emphasize the importance of taking and measuring samples from the parts of various oxidation degrees in a lava flow.

Key words: chemical remanent magnetization, Hawaii, igneous rock, oxidation, palaeointensity, titanomagnetite.

1 INTRODUCTION

The complete restoration of the ancient geomagnetic field requires absolute palaeointensities together with the field directions. As natural remanent magnetization (NRM) of volcanic rocks generally originates from thermoremanent magnetization (TRM), comparison of NRM with TRM given in a laboratory field can yield an absolute palaeointensity, assuming a linear law for the TRM. There are two major methods to determine the palaeointensity: the Thellier method (Thellier & Thellier 1959) and the Shaw method (Shaw 1974).

The Thellier method and its modified version by Coe (1967) have been considered as the most reliable palaeointensity determination. However, there are some problems in obtaining accurate palaeointensities whatever method we apply. One is a non-ideal behaviour of multidomain (MD) components. Levi (1977) reported that the Thellier method with MD magnetites resulted in non-linear (concave-up) trends on Arai diagrams and their lower blocking temperature portions led to apparently high palaeointensities. This MD effect was confirmed by Xu & Dunlop (1995) since the degree of convexity increased with grain size in their studies.

There is another serious problem, namely thermochemical remanent magnetization (TCRM). TCRM is acquired by grain growth of new magnetic minerals below their Curie temperatures and can be a part of NRM during initial cooling of volcanic rocks. Kellogg *et al.* (1970) studied the TCRM effect on palaeointensity determination, applying the Thellier method to basaltic samples from northern New Mexico. They suggested that the palaeointensity experiments could give reasonable values even if TCRM shared a considerable part of the NRM. However, Tanaka & Kono (1991) obtained an anomalous palaeointensity from the Hawaiian 1960 lava in the Big Island of Hawaii using Coe's version of the Thellier method. This result gave a 48 per cent stronger value than expected, despite satisfying all the strict criteria. Several authors (Mankinen & Champion 1993; Tsunakawa & Shaw 1994) have mentioned that TCRM might be a source of the erroneous results of the Hawaiian 1960 lava. Therefore,

in the present study, we will examine the possibility that TCRM is a possible source of erroneous palaeointensities. Experiments using the Thellier method have been carried out.

The advanced type Shaw method (LTD–DHT Shaw method, see below) has also been applied for a comparative study, even though its original version has been criticized mainly because of its poor theoretical background. The most severe critique against the Shaw method is its laboratory heating above the Curie temperature, which usually changes the TRM acquisition capacity of samples. Corrections using the anhysteretic remanent magnetization (ARM) in the modified Shaw method (Kono 1978; Rolph & Shaw 1985) have not been well studied theoretically except for a few reports (e.g. Tanaka 1999) and sometimes lead to an erroneous palaeointensity. Kono (1987) showed that the ARM correction would give a different palaeointensity by up to 40 per cent for some recent basalt by 300 min of laboratory heating. Vlag *et al.* (2000) pointed out that the ARM correction by Rolph & Shaw (1985) might not be valid for the laboratory transformation of Ti-rich titanomagnetite into a magnetite–ilmenite intergrowth because of insensitivity of ARM coercivity spectra to the transformation. Comprehensive reviews of the global palaeointensity database published recently did not accept the results by the Shaw method (e.g. Juarez & Tauxe 2000; Selkin & Tauxe 2000; Tarduno *et al.* 2001).

Most of the previous Shaw-type measurements have been performed with a single laboratory heating. There have been, however, some studies on improvement of the Shaw method. Tsunakawa & Shaw (1994) proposed the double-heating technique for the Shaw method (DHT Shaw method), which can test the validity of the ARM correction for individual samples by heating them twice. They applied this technique to some lava flows with known palaeofields. The samples passing the double-heating test, except for one, showed good agreement with the expected values within a 10 per cent difference. For the Hawaiian 1960 lava, they rejected two erroneously high intensities by this technique and successfully obtained an appropriate value of 34.5 μT. Tanaka *et al.* (1997) also reported on the validity of the double-heating test in the Shaw method.

The Hawaiian 1960 lava yielded both reasonable and anomalous palaeointensities in the previous studies, although it is typical of hotspot basalts commonly used for absolute palaeointensity studies. In the present study, we have performed systematic palaeointensity determinations on this lava in order to examine possible causes of its anomalous behaviour. The methods applied are Coe's version of the Thellier method (Coe 1967) and the double-heating technique of the Shaw method combined with low-temperature demagnetization (LTD–DHT Shaw method; Tsunakawa *et al.* 1997; Tsunakawa & Yamamoto 1999). The LTD is also conducted in the Thellier method at each temperature step for some specimens to evaluate the effect of multidomain components. Although the validity of AF cleaning in the Thellier experiment has not been conclusive in some previous studies (e.g. Coe & Gromme 1973; Roperch *et al.* 1988), the LTD–Thellier experiment seems to be useful for such a purpose, because the LTD is known as an effective technique for demagnetizing MD-like components exclusively (e.g. Ozima *et al.* 1964; Heider *et al.* 1992). Microscopic observations and measurements of hysteretic parameters are further performed to clarify the relationship between the rock magnetic properties and the resultant palaeointensities.

2 SAMPLES

We collected palaeomagnetic core samples from the Hawaiian 1960 lava flow using a portable engine drill in March of 1998. All the samples were orientated using both the sun and magnetic compasses. The sampling site is a roadcut of the exposed lava approximately 4 m in thickness and approximately 15 m in width (19°30.43′N, 154°50.46′W). As the core positions were separated into four subsites (Fig. 1), their sample IDs were named A-1–A-5, B-1–B-7, B-8–B-10 and C-1–C-4 with reference to their rock magnetic properties described in the next section. Each core was cut into several sister specimens in order to apply the Thellier and the LTD–DHT Shaw methods. The expected field intensity is 36.2 μT from the DGRF 1965.

The palaeointensities of this lava have already been measured in previous studies. Tanaka & Kono (1991) obtained 48 per cent higher field intensity from one out of five successful results, whereas another four specimens gave a good average of 37.0 ± 3.9 μT. Tsunakawa & Shaw (1994) reported an intensity of 34.5 μT from one specimen by the DHT Shaw method, while the other two specimens did not pass their selection criteria. Valet & Herrero-Bervera (2000) compared the coercivity spectra between NRM and TRM without the ARM correction and gave an average of 41.1 μT from seven out of 10 specimens.

Systematic palaeointensity measurements have also been performed by Hill & Shaw (2000). They applied the microwave method to the samples from two vertical sections of the lava. One section exhibited a good linear behaviour on the Arai plots with a mean palaeointensity of 33.0 ± 3.9 μT ($N = 20$), but the other section showed an anomalous two-slope behaviour, resulting in a mean value of 43.4 ± 9.7 μT ($N = 15$) when the first slopes were adopted. They mentioned that this behaviour was similar to that noted by Tanaka & Kono (1991), and attributed it to NRM containing high-temperature CRM rather than MD behaviour because their samples exhibited ideal linear NRM/T_MRM (T_MRM; microwave-induced

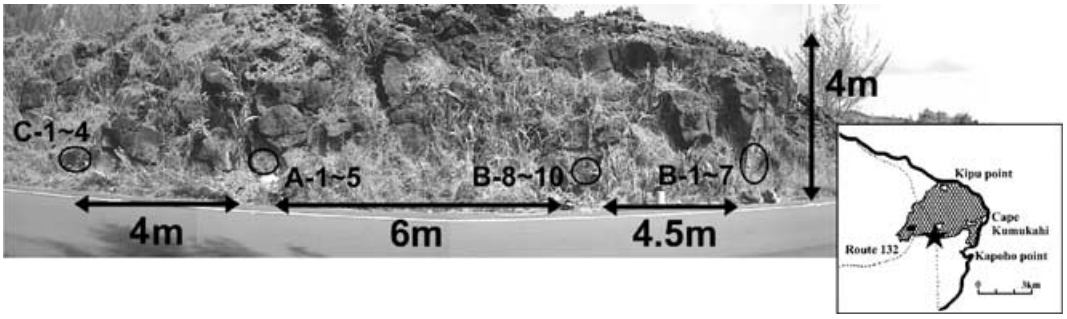

Figure 1. Sampling site of the Hawaiian 1960 lava. The palaeomagnetic cores were collected from four subsites and their IDs are named A-1–5, B-1–7, B-8–10 and C-1–4 with reference to their rock magnetic properties (see the text). In the lower right-hand figure, a solid star shows the sampling location (19°30.43′N, 154°50.46′W). The daubed area and hatched region indicate the scoria cone and flow of the 1960 lava, respectively (after the geological map of the island of Hawaii compiled by Wolfe and Morris).

thermoremanent magnetization) plots for simulated NRM of the laboratory-applied T_MRM. They also mentioned that the correct answer was obtained by averaging the two slopes. However, the physical background of this averaging is not clear because the Thellier method theoretically requires a constant NRM/TRM ratio for different blocking temperatures.

Compiling the palaeointensities reported so far, they range from 27.0 to 68.7 μT.

3 ROCK MAGNETIC PROPERTIES

Since LTD is known as the effective technique for demagnetizing MD-like components and extracting single-domain (SD)-like remanences of titanium-poor titanomagnetite (e.g. Ozima *et al.* 1964; Heider *et al.* 1992), it is useful for separating SD- and MD-like coercivity spectra of remanences. Therefore, we applied this technique to the ARM of the specimens (the detailed LTD procedure is described in Section 4.2). Based on the resultant coercivity spectra of ARM, the four subsites can be classified into three rock magnetic groups of A (sample ID of A-1–5), B (B-1–10) and C (C-1–4). Their averaged patterns of the surviving (SD-like) and demagnetized (MD-like) components by LTD are illustrated in Figs 2(a)–(c).

Thermomagnetic analyses were carried out for representative samples of each rock magnetic group in helium gas flow by a vibrating sample magnetometer (MicroMag 3900 VSM, Princeton Measurement Corporation). All of the samples had a similar main

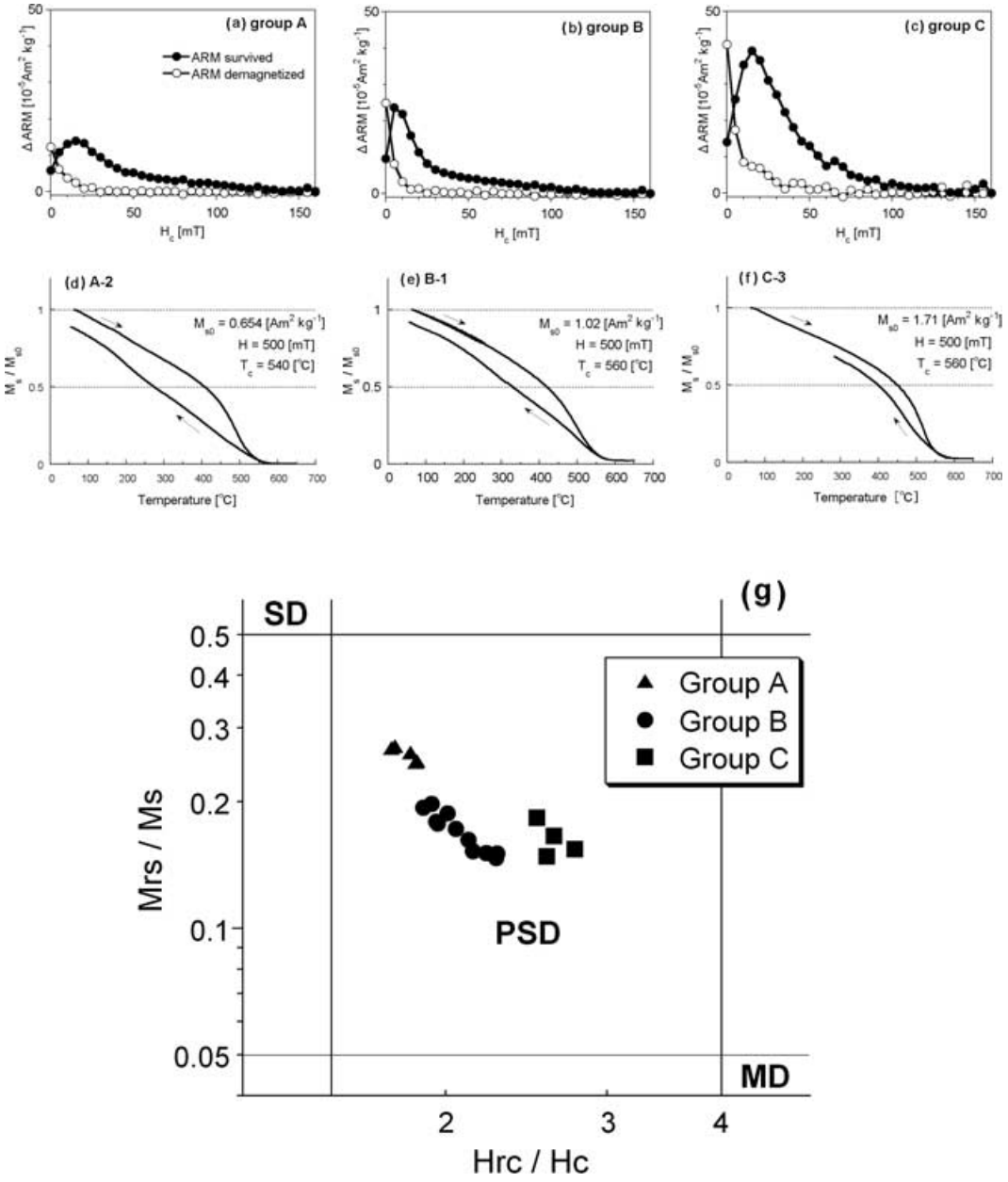

Figure 2. Results of the rock magnetic experiments. (a)–(c) Averaged patterns of the ARM coercivity spectra survived and demagnetized by LTD for each rock magnetic group. The vertical axis indicates a difference of ARM between adjacent coercivities while the horizontal axis indicates coercivity. (d)–(f) The measured thermomagnetic curves for each group. The vertical axis indicates a normalized saturation magnetization in a DC field of 0.5 T. The measurement of C-3 was stopped at 275 °C in the cooling. (g) Day plot for all the measured cores. The coordinates are logarithmic. The data points resulted from averages for five small chips of each core.

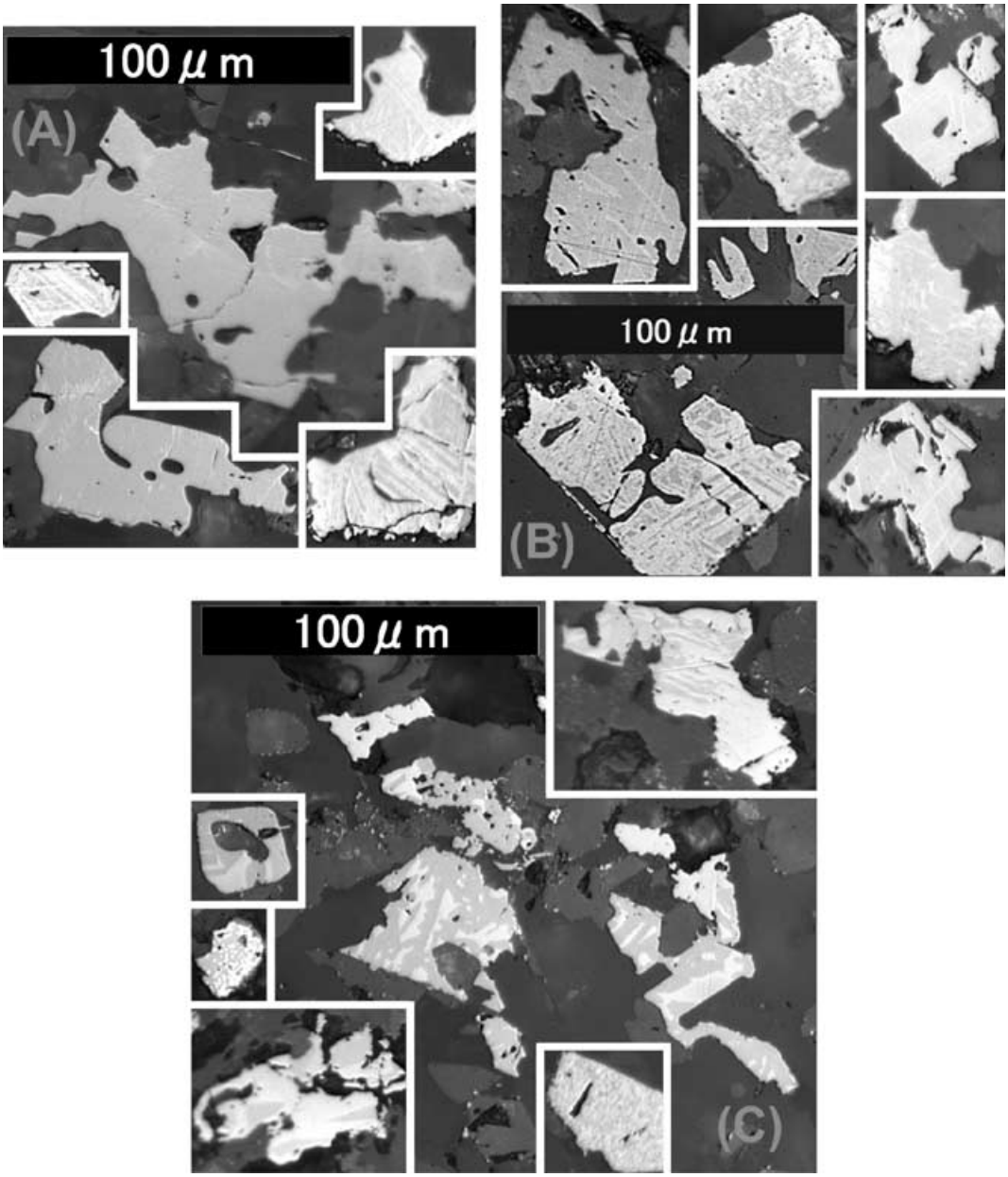

Figure 3. Reflected light microscopy of the opaque minerals for each rock magnetic group. (a) Oxidation index of I–III for group A, (b) II–IV for B and (c) IV–VI for C. The black bar indicates a scale of 100 μm.

phase that corresponds to titanium-poor titanomagnetite with $x \sim 0.05$ (Figs 2d–f). Therefore, the LTD treatment is probably effective for erasing MD components of the present samples (e.g. Ozima *et al.* 1964; Heider *et al.* 1992). We also measured hysteresis properties of saturation magnetization (M_s), remanent saturation magnetization (M_{rs}), coercivity (H_c) and remanent coercivity (H_{rc}) for five small chips from each of the palaeomagnetic core. The Day plot (Day *et al.* 1977) shows clusters corresponding to each rock magnetic group in Fig. 2(g). Although all the points are plotted in the pseudo-single-domain (PSD) area, MD-like components are considered to decrease in the order of groups C, B and A. This order is supported from the ratio of the LTD demagnetized components to the LTD-surviving components for ARM (Figs 2a–c). These MD-like components are, however, considered to be not so large in NRM because the total amount of NRM demagnetized by LTD was less than 13 per cent.

Several samples from each group were also observed by a microscope with reflected light (Fig. 3). In the observation, it is noted that there are many pseudobrookites in group C. Following Wilson & Watkins (1967), high-temperature oxidation indices were defined as follows.

(i) Homogeneous titanomagnetite.

(ii) Titanomagnetite containing a few ilmenite lamellae.

(iii) Titanomagnetite with abundant ilmenite lamellae.

(iv) Titanomagnetite shows signs of incipient alteration to titanohematite.

(v) Both ilmenite and titanomagnetite are oxidized to rutile, although some relic areas of titanomagnetite may exist.

(vi) Maximum degree of oxidation characterized by the high-temperature index mineral pseudobrookite.

The dominant phases were recognized to be classes II, III and VI for groups A–C, respectively. Taking other minor phases into account, we identify these oxidation indices as I–III, II–IV and IV–VI, respectively. This classification was supported by the observations with an electron probe microanalyser (EPMA) in Fig. 4, and by the total intensities of ARM prior to the laboratory heating. The ARM intensities clearly increased in order of groups A–C. It is consistent with the observations by Watkins & Haggerty (1967) that there is a positive relationship between the magnetization intensity and the degree of oxidation. Hence the deuteric oxidation is considered to

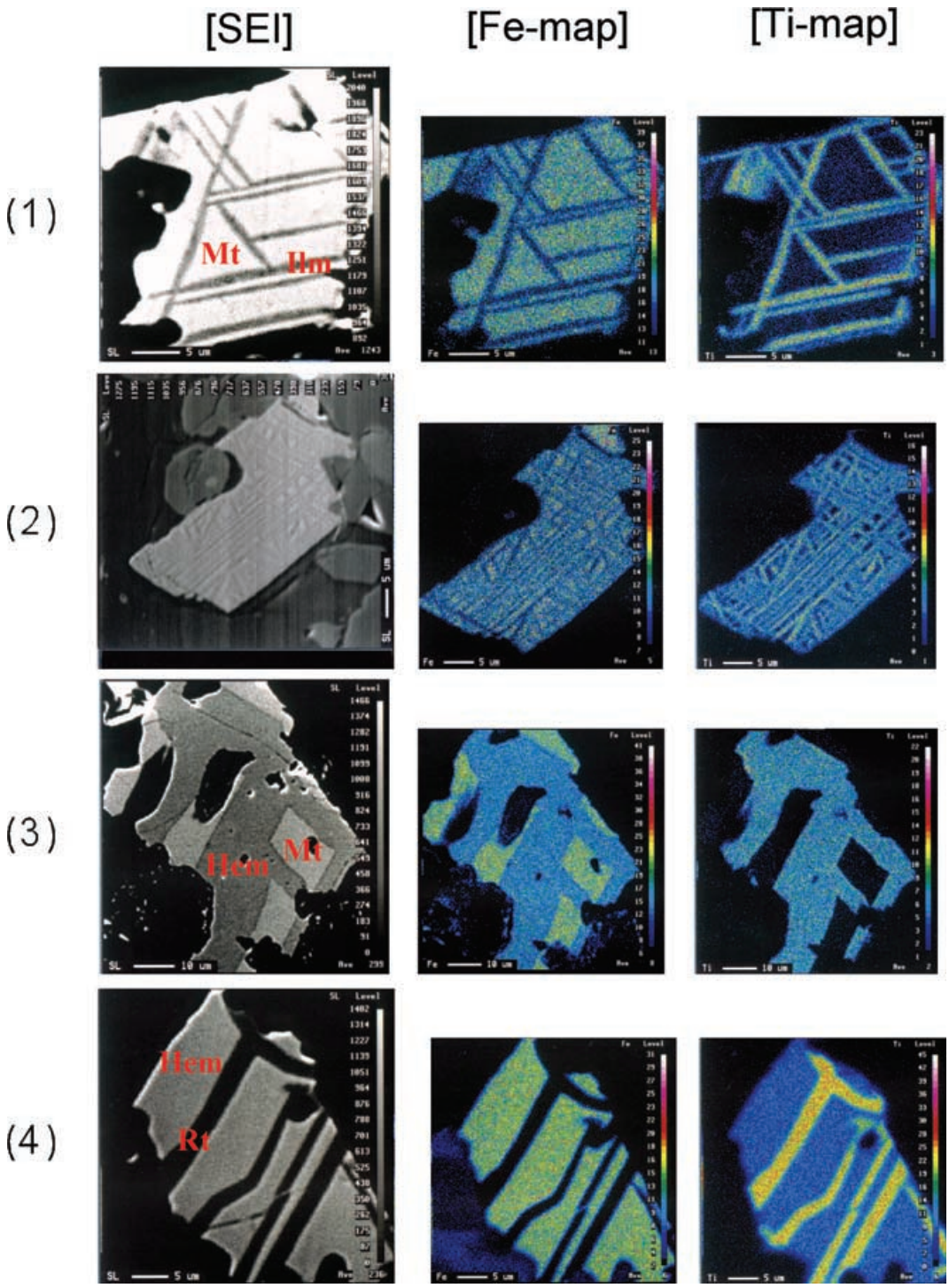

Figure 4. EPMA photographs of the representative magnetic minerals in (1) B-1, (2) A-2 and (3, 4) C-3. The oxidation index is identified to be (1) II, (2) III, (3) IV and (4) VI. The left-hand, middle and right-hand columns are secondary electron images (SEI), maps of Fe and Ti, respectively. Labels are as follows; Mt: titanomagnetite, Ilm: ilmenite, Hem: titanohematite, Rt: rutile.

progress in the order of A–C. This can be explained by the fact that higher degrees of deuteric oxidation produce titanium-poor titanomagnetites.

4 PALAEOINTENSITIES

4.1 Coe's version of the Thellier method

Coe's version of the Thellier method (Coe 1967) was applied to 19 specimens. They were subjected to stepwise heating at 20–50 °C intervals up to 600 °C in air for 1–1.5 h with an electric furnace (Natsuhara–Giken TDS-1). As we held the top temperature as briefly as possible in order to avoid sample alteration, the hold time was taken to be 6 min. The reproducibility of the top temperature was better than ±1 °C. TRM was given in a 30 μT DC field at each step, and all the remanent magnetizations were measured by a spinner magnetometer (Natsuhara–Giken SMD-88) with a resolution of better than $\pm 10^{-8}$ A m^2. The experimental results are judged by the following selection criteria.

(1) The primary component of NRM is recognized in the orthogonal plot of thermal demagnetization.

(2) The linear portion of the primary component in the Arai diagram is not less than 15 per cent of the original NRM. This portion is defined by a number of data points ($N \geq 5$), and is in the range of acceptable temperature intervals in the pTRM test.

(3) In the pTRM test, the repeat pTRM is not significantly different from the first pTRM at a 2σ level. This σ is calculated from the errors arising from the magnetization measurements and the temperature and applied field controls.

The results are discarded unless they satisfied all the criteria. These criteria are almost the same as Coe's (Coe *et al.* 1978), but are more stringent in terms of the number of data points. Magnetic susceptibilities were also measured at each step with a susceptibility magnetometer (Bartington MS2) as another monitor of the sample alteration in the laboratory heating. Their changes, however, did not exceed ±10 per cent of the original values in all cases.

The obtained results are summarized in Table 1 with a correlation coefficient (r), a quality factor (q; Coe *et al.* 1978) and NRM fraction (f) of the linear portions. Results of the two samples (A-4-3 and B-10-1) were discarded because both of them failed the pTRM test below 350 °C and their NRM fractions do not satisfy the above condition (2). Consequently, the remaining 17 samples gave palaeointensities ranging from 36.0 to 69.0 μT. The overall average of 49.0 ± 9.6 μT is approximately 35 per cent higher than expected. According to the rock magnetic classification, these results are described below for each group. Their representative Arai diagrams are also shown in Figs 5(a)–(c).

Group A

A positive pTRM test was observed up to 450–500 °C for four out of five specimens. Their linear portions are composed of 29–50 per cent of NRM, resulting in an average palaeointensity of 41.9 ± 4.2 μT. This is slightly higher than expected.

Table 1. Experimental results by the Thellier method.

Specimen	NRM_0 (10^{-5} A m^2 kg^{-1})	PTRM	T_1–T_2	N	r	q	f	Slope	F (μT)
A-1-3	173	20–500	250–500	7	0.987	5.10	0.455	1.51 ± 0.11	45.3**
A-2-3	172	20–500	165–500	8	0.997	11.4	0.477	1.39 ± 0.05	41.7
A-3-3	229	20–500	20–500	8	0.995	9.90	0.498	1.20 ± 0.05	36.0
A-4-3	227	–	–	–	–	–	–	–	–
A-5-3	211	20–450	20–450	6	0.991	3.45	0.288	1.48 ± 0.10	44.4*
B-1-3	330	20–500	20–475	7	0.987	5.88	0.513	2.05 ± 0.15	61.5**
B-2-1	332	20–500	250–500	7	0.998	14.3	0.474	1.63 ± 0.04	48.9
B-3-3	342	20–500	300–500	6	0.997	10.1	0.476	1.97 ± 0.07	59.1
B-4-3	312	20–580	250–475	6	0.996	6.41	0.359	2.30 ± 0.10	69.0
B-5-1	323	20–500	20–500	8	0.998	16.6	0.516	1.82 ± 0.05	54.6
B-6-3	321	20–570	165–570	10	0.997	27.5	0.947	1.60 ± 0.05	48.0
B-7-3	402	20–540	250–520	8	0.988	8.08	0.609	2.11 ± 0.13	63.3**
B-8-1	142	20–540	250–520	8	0.991	8.86	0.579	1.73 ± 0.10	51.9**
B-9-3	146	20–500	250–500	7	0.998	13.4	0.465	1.59 ± 0.05	47.7
B-10-1	163	20–350	–	–	–	–	–	–	–
C-1-3	352	20–600	20–600	13	0.999	76.3	0.988	1.33 ± 0.01	39.9
C-2-3	583	20–600	20–600	13	0.999	47.0	0.966	1.49 ± 0.02	44.7
C-3-3	521	20–600	20–600	13	1.00	98.0	0.981	1.36 ± 0.01	40.8
C-4-1	249	20–580	20–580	11	0.999	44.1	0.921	1.23 ± 0.02	36.9
A-4-4L	209	20–450	20–425	5	0.989	2.60	0.301	2.85 ± 0.24	85.5*
B-9-4L	129	20–500	20–425	5	0.999	9.53	0.286	2.72 ± 0.06	81.6
C-4-4L	367	20–600	250–560	10	0.999	45.9	0.873	1.25 ± 0.02	37.5

NRM_0, NRM intensity; PTRM, acceptable temperature intervals in the pTRM test; T_1–T_2, N, temperature intervals and number of the data included in the linear segments; r, q, f, correlation coefficient, quality factor and NRM fraction of the linear NRM–TRM portion in the Arai diagram; slope, slope of the linear NRM–TRM fraction; F, calculated palaeointensity. TRM was induced in a laboratory DC field of 30.0 μT. A-4-4L, B-9-4L and C-4-4L are the results of the LTD version (see the text).

*Rejected if the additional selection criterion of $q \geq 5$ is applied.

**Rejected if the additional selection criteria of $q \geq 5$ and $r \geq 0.995$ are applied.

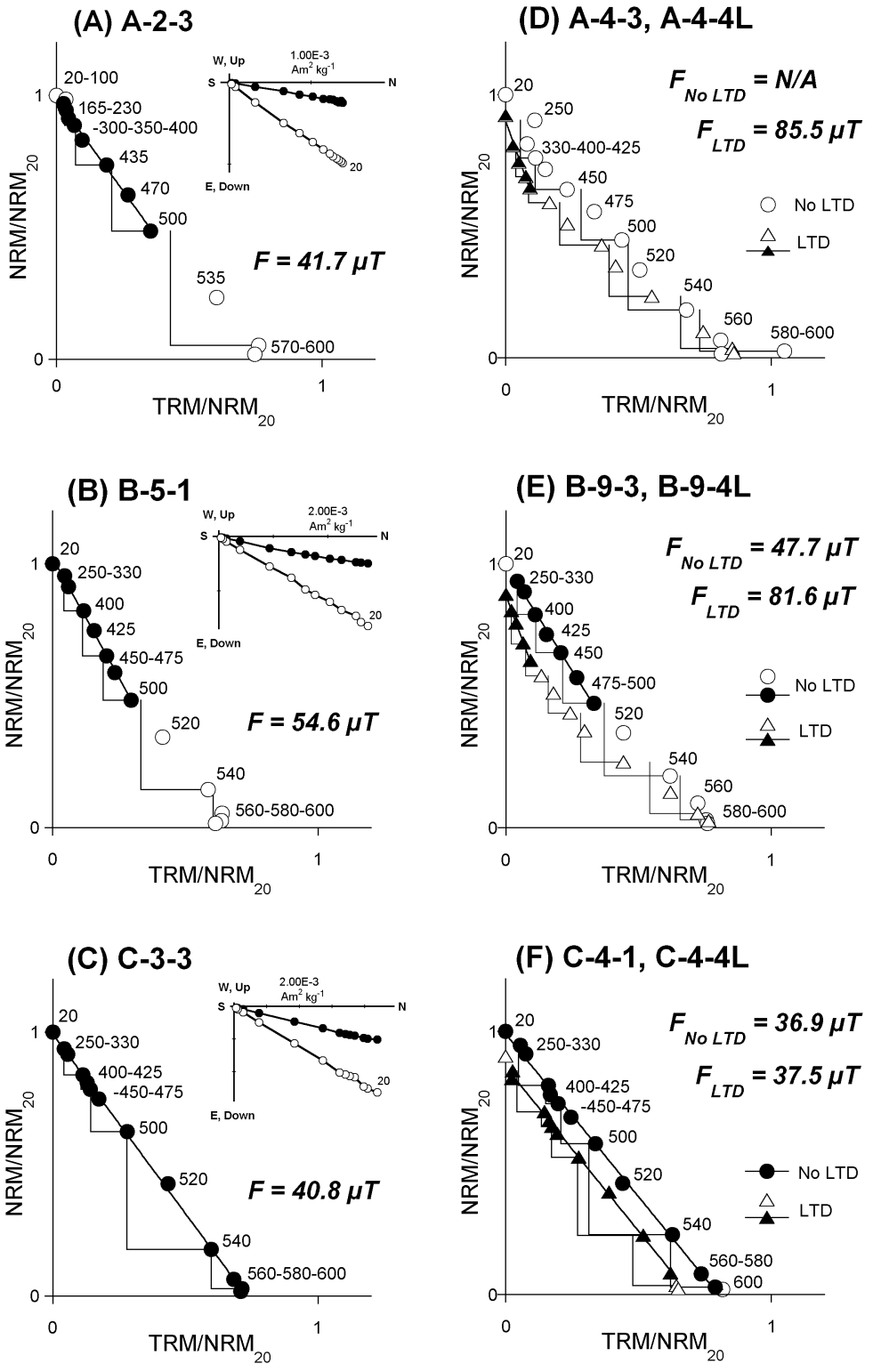

Figure 5. Results of the Thellier experiments. (a)–(c) Representative results for each rock magnetic group. Linear portions consist of closed symbols. (d)–(f) Experimental results by the Thellier method with and without the LTD treatment for each group. In these figures, the LT memories of NRM and TRM are plotted. The temperature steps are the same in both versions.

Group B

Successful results were obtained from nine out of 10 specimens and all of them yielded palaeointensities higher than 47 μT. The linear portions, consisting of 36–95 per cent of the NRMs, give an average intensity of 56.0 ± 7.6 μT ($N = 9$) which is 55 per cent higher than expected. They passed the pTRM test up to 500–580 °C, but NRM fractions (f) for them are around 0.6. Therefore, some thermal alteration probably occurred during the laboratory heating at high temperatures.

Group C

All the specimens show good linearity extending to the high blocking temperature portions. Thus they have the best quality factors ($q >$ 47) among the groups. The linear portions are composed of more than 90 per cent of their NRMs and an average palaeointensity is calculated to be 40.6 $\pm$ 3.2 μT ($N = 4$).

The average intensities of groups A and C are concordant with the expected value to a 2σ (σ is the standard deviation) level, while that of group B is significantly larger. In group B, the standard deviation (1σ) is 14 per cent of the mean, indicating a relatively good result of internal consistency, i.e. the multispecimen test. If we do not know either the expected field intensity or the data from other subsites, the higher average of 56.0 μT may be regarded as representative. This suggests that it is very important to collect and measure samples with various rock magnetic properties from a single lava flow.

One may consider that the erroneous palaeointensities can be excluded by more stringent selection criteria, although no definite criteria have been established. If a crucial condition of $q \geq 5$ is adopted, only one result of A-5-3 (44.4 μT) is rejected (Table 1). The correlation coefficient is another candidate as a crucial criterion, for example, $r \geq 0.980$ in Tanaka *et al.* (1995) and Laj *et al.* (2002). If we adopt the further stringent criteria of $q \geq 5$ and $r \geq 0.995$, they screen the results of A-1-3 (45.3 μT) and A-5-3 (44.4 μT) for group A and B-1-3 (61.5 μT), B-7-3 (63.3 μT) and B-8-1 (51.9 μT) for group B. This drastically changes the overall success rate, decreasing it to be 12/19, but the mean intensity of group B is still at a higher value of 54.6 $\pm$ 8.4 μT. If the condition of $r \geq 0.999$ is applied, only the palaeointensities from group C survive and then give a reasonable average. These results indicate that the usual selection criteria do not work well to discriminate inappropriate data for the Hawaiian 1960 lava. Such a failure of the criteria does not seem to be a peculiar case of the Hawaiian 1960 lava. Calvo *et al.* (2002) also reported abnormal intensities from 1910 and 1928 Mt Etna basalts in spite of strict reliability criteria being applied.

4.2 LTD–DHT Shaw method

We applied the LTD–DHT Shaw method (Tsunakawa *et al.* 1997; Tsunakawa & Yamamoto 1999) to the sister specimens from the 19 cores used in the Thellier experiment. The procedure of the method is shown in Fig. 6. It has the following additional treatments compared with the previous DHT Shaw method (Tsunakawa & Shaw 1994).

(1) NRM, TRM1 and TRM2 are subjected to LTD and their LT memories are measured.

(2) For ARM, the AF demagnetization is first conducted before the LTD treatment (ARM00, ARM10 and ARM20). Then the same

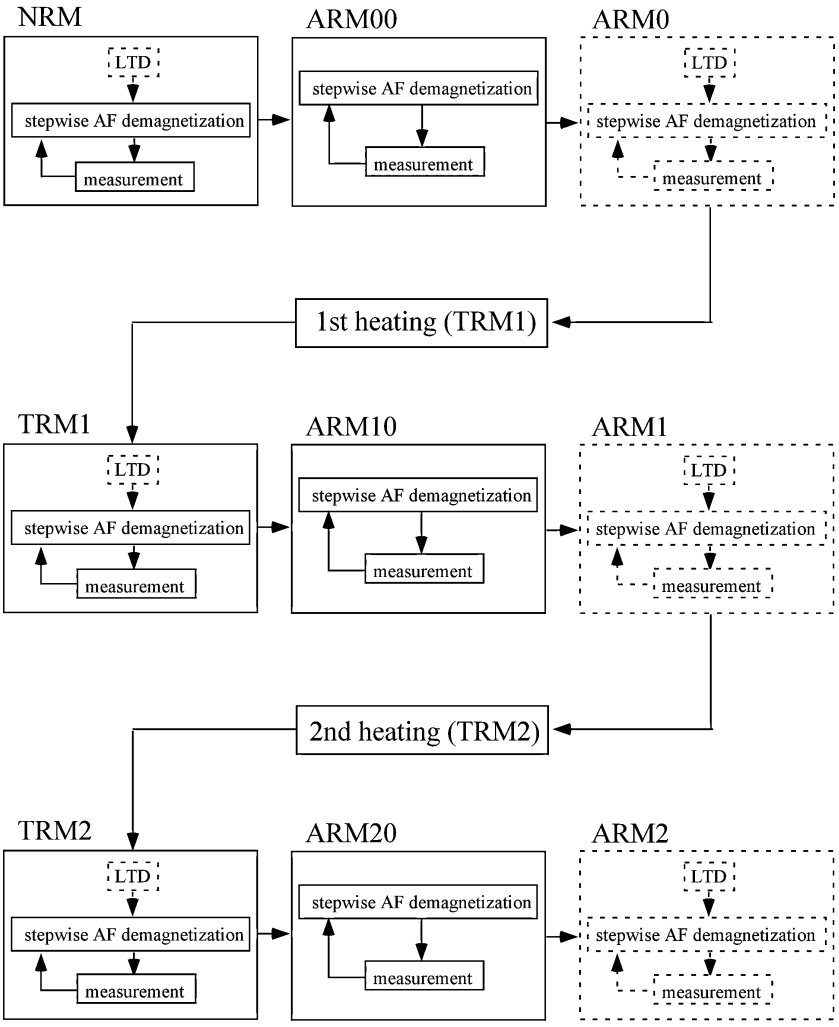

Figure 6. Experimental procedures of the LTD–DHT Shaw method (Tsunakawa *et al.* 1997; Tsunakawa & Yamamoto 1999). This method employs some additional procedures as indicated by the dotted-line box when compared with the previous double-heating technique (Tsunakawa & Shaw 1994).

ARM is given again and subsequently subjected to LTD and AF demagnetization (ARM0, ARM1 and ARM2).

(3) For the LTD treatment, the specimens are soaked into liquid nitrogen in a plastic bottle for 10 min. This bottle is placed in a magnetically shielded case where a residual field is less than 100 nT. Taken from the bottle, the specimens are warmed up to room temperature in the same case for approximately 60 min.

The AF demagnetization was carried out at 5 or 10 mT intervals up to a peak field of 160 mT, sometimes up to 180 mT. All the specimens were heated twice at 610 °C in the electric furnace for 10 min in the first heating (TRM1) and 20 min in the second heating (TRM2), applying a DC field of 30 μT to give a whole TRM. In the experiment, most specimens were heated in air while two (A-5-2N and B-6-1N) were heated in nitrogen gas flow. ARM was given in a 100 μT DC field parallel to NRM or TRM, associated with an AF of 160 or 180 mT. All the remanence measurements and the AF demagnetizations were performed by an automatic spinner magnetometer (Natsuhara–Giken DSPIN-2; Kono *et al.* 1984, 1997) with a resolution of better than $\pm 10^{-7}$ A m^2. The total time for demagnetization and measurement of a specimen was approximately 1 h.

All the magnitudes of remanences were calculated from vector subtraction between the measured and maximum AF step. For instance, if the maximum AF step is 160 mT, NRM[H_c] is calculated by subtracting NRM after a 160 mT AF cleaning from that after an AF cleaning of $H = H_c$. This is because the maximum AF demagnetizing field does not necessarily erase all the remanent magnetizations, as stated in Rolph & Shaw (1985). The ARM correction was applied to TRM1 and TRM2 in the following way (Rolph & Shaw 1985):

$$\mathrm{TRM1}^* = \mathrm{TRM1} \times \frac{\mathrm{ARM0}}{\mathrm{ARM1}}$$

$$\mathrm{TRM2}^* = \mathrm{TRM2} \times \frac{\mathrm{ARM1}}{\mathrm{ARM2}}$$

where TRM1, TRM2, ARM0, ARM1 and ARM2 are the remanence magnitudes at each AF step. This correction was tested in the second heating experiment for the individual specimens. The experimental results are judged by the following selection criteria similar to the Thellier method.

(1) The primary component of NRM is recognized in the orthogonal plot of AF demagnetization.

(2) The linear portion in the NRM-TRM1* diagram, which should consist of the primary component of relatively high coercivity, is not less than 15 per cent of the original NRM ($f_N \geq 0.15$). The linear portion is defined by the correlation coefficient ($r_N \geq 0.995$) and the number of data points ($N \geq 5$).

(3) The linear portion in the TRM1–TRM2* diagram is determined in the same way as in the above ($r_T \geq 0.995$, $N \geq 5$). This fraction is not less than 15 per cent of the original TRM1 ($f_T \geq 0.15$).

(4) The slope of the linear portion in the TRM1–TRM2* diagram is in the range of 1.00 ± 0.05, because the representative experimental error is estimated to be ±5 per cent in the present study.

The obtained results are summarized in Table 2 and shown in Fig. 7 for their representatives. The successful palaeointensities range from 31.2 to 52.8 μT. In spite of the low success rate of 9/19, the average of 39.4 ± 7.9 μT is improved when compared with the

Table 2. Experimental results by the LTD–DHT Shaw method.

Specimen	First heating					Second heating					F
	H_L	slope $_A$	slope $_N$	f_N	r_N	H_L	slope $_A$	slope $_T$	f_T	r_T	(μT)
A-1-2	0	0.827	0.845	1.00	0.996	0	0.847	*1.08*	1.00	1.00	–
A-2-1	0	1.07	1.12	1.00	0.996	0	0.901	1.05	1.00	0.999	33.6
A-3-2	35	1.24	1.58	0.536	*0.981*	0	0.956	1.03	1.00	0.999	–
A-4-2	55	1.27	1.10	0.338	0.995	0	0.822	1.01	1.00	0.999	33.0
A-5-2N	35	1.26	1.33	0.526	0.998	0	0.961	1.03	1.00	1.00	39.9
B-1-1	25	1.01	1.62	0.458	*0.992*	0	1.03	1.03	1.00	0.999	–
B-2-2	30	0.850	1.23	0.388	0.995	0	0.907	0.989	1.00	1.00	36.9
B-3-1	25	1.03	1.67	0.478	*0.991*	0	0.924	*1.11*	1.00	1.00	–
B-4-2	20	1.00	1.76	0.582	0.997	0	0.969	1.01	1.00	0.999	52.8
B-5-2	35	0.966	2.12	0.467	0.997	0	0.949	*1.09*	1.00	0.999	–
B-6-1N	45	1.09	1.72	0.382	0.997	45	0.898	*1.28*	0.281	0.998	–
B-7-1	30	0.985	2.15	0.491	*0.994*	0	0.931	1.05	1.00	0.999	–
B-8-3	35	0.815	1.15	0.351	0.995	0	0.891	*0.933*	1.00	0.999	–
B-9-1	35	1.01	1.83	0.363	*0.984*	0	0.953	1.02	1.00	0.999	–
B-10-2	20	0.733	1.04	0.566	0.995	0	0.832	0.958	1.00	1.00	31.2
C-1-2	5	0.847	1.18	0.962	0.999	40	1.12	0.954	0.294	0.998	35.4
C-2-2	5	0.844	1.73	0.971	0.999	10	1.04	0.968	0.825	1.00	51.9
C-3-2	10	0.889	1.32	0.860	0.999	30	1.13	1.01	0.420	0.998	39.6
C-4-2	5	0.774	1.13	0.958	0.997	50	1.06	*1.20*	0.210	0.994	–

H_L, the lowest coercivity force taken for the linear segments; slope$_A$, slopes of ARM spectra ($\geq H_L$) before and after the heating; slope$_N$, slope$_T$, slopes of the linear segments in the NRM–TRM1* and TRM1–TRM2* diagrams; r_N, r_T, correlation coefficients of the linear NRM–TRM1* and TRM1–TRM2* segments; f_N, f_T, NRM and TRM1 fractions of the linear NRM–TRM1* and TRM1–TRM2* segments; F, calculated palaeointensity. TRM was induced in a laboratory DC field of 30.0 μT. 'N' denotes the specimens heated in nitrogen gas flow. Italic numbers are indicated to be out of the selection criteria.

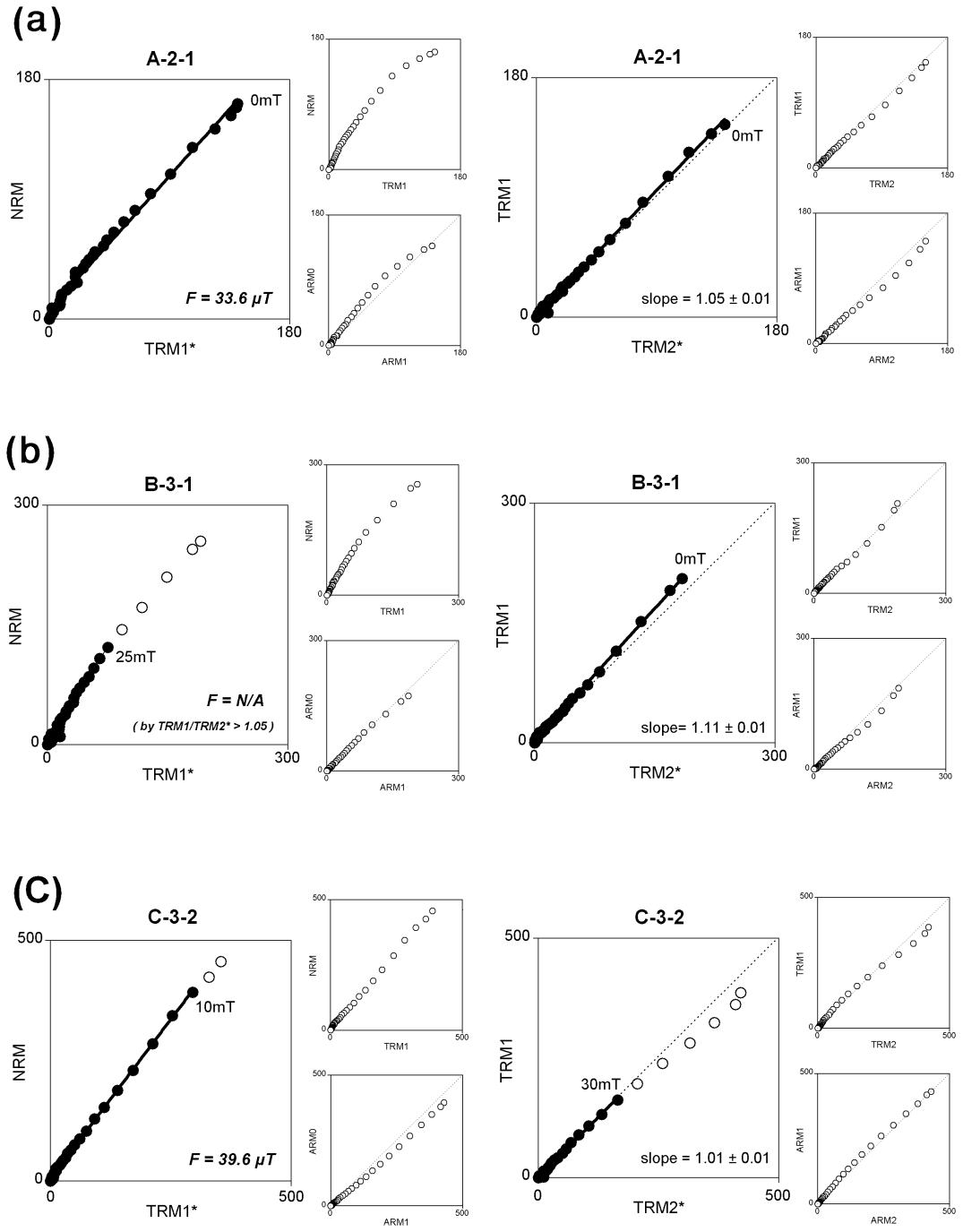

Figure 7. Representative results by the LTD–DHT Shaw method for (a) group A, (b) group B and (c) group C. Solid symbols indicate the linear portion. The result of B-3-1 is rejected because the slope in the TRM1–TRM2* diagram is greater than 1.05.

Thellier results. The major reasons for such a low success rate are that: (1) the linear portions are not detected in the NRM–TRM1* diagrams ($r_N < 0.995$) and (2) the slopes of the linear portion in the TRM1–TRM2* diagrams are out of 1.00 ± 0.05. It is easily seen that the two palaeointensities of B-4-2 (52.8 μT) and C-2-2 (51.9 μT) are much higher than the others (31.2–39.9 μT). Thus the standard deviation (7.9 μT, 20 per cent) is not small. If these two are excluded as outliers, the standard deviation becomes significantly smaller (9 per cent) with the corresponding average of 35.7 ± 3.3 μT ($N = 7$). This average value is quite consistent with the expected one.

From these results, we state that the ARM correction plays an important role in obtaining appropriate palaeointensities. This is because the palaeointensities are not necessarily obtained from the samples with $\text{slope}_A = 1$. In Fig. 8, the relationship between palaeointensities (F/F_e) and ARM correction degrees (ARM0/ARM1) is shown for the nine successful samples. It is recognized that we obtained good palaeointensities for a relatively wide range of ARM0/ARM1 ratios. This indicates that the ARM correction is meaningful in the LTD–DHT Shaw method. Valet & Herrero-Bervera (2000) obtained reasonable palaeointensities from the Hawaiian 1960 lava by a simple ratio of NRM/TRM without the

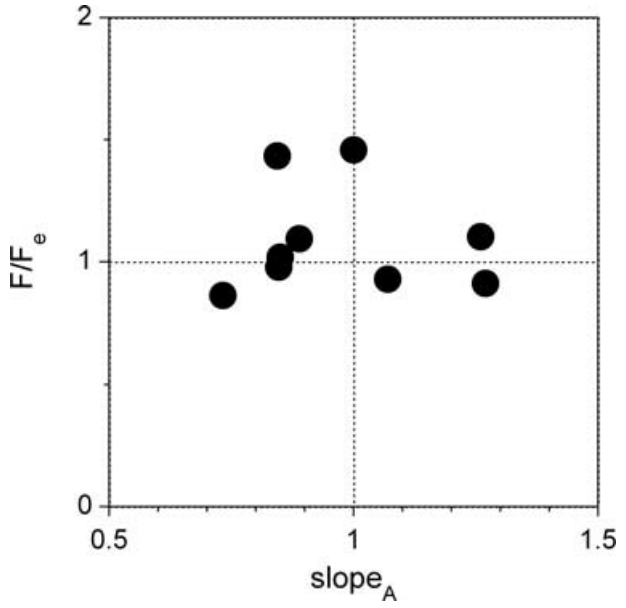

Figure 8. Relation between the obtained palaeointensities (F) and corresponding slopes of ARM spectra for the first laboratory heating (slope$_A$) in the LTD–DHT Shaw method. The palaeointensities are obtained from a relatively wide range of the slope$_A$, indicating that the ARM correction is meaningful in this method. Note that the palaeointensities are normalized by the expected value (Fe = 36.2 μT).

ARM correction, but our results suggest that they were fortuitous to have had unit slope$_A$ (if measured) for all samples they used.

5 DISCUSSION

5.1 Causes for the high palaeointensities

In the present study, erroneously high palaeointensities were yielded especially from the specimens of group B using the Thellier method. This is very surprising because these samples have ordinary rock magnetic properties for the palaeointensity studies. In this section, five possible reasons for the high palaeointensities are examined: (1) terrain effect, (2) multidomain components, (3) pseudo-single-domain components, (4) thermochemical remanent magnetization production in the laboratory and (5) TCRM production in initial cooling.

Terrain effect

Baag *et al.* (1995) measured the ambient geomagnetic field above recent basalts on the island of Hawaii. According to their observations, the local magnetic field directions are substantially different from the IGRF by up to 20° except for those composed of shelly pahoehoe and a flat thin lava pond. This suggests that we should pay attention to the local terrain effect for a precise palaeomagnetic study. In this study, however, the local magnetic anomaly is unlikely to be the main cause for the anomalous palaeointensities because of the following reasons.

(1) According to the aeromagnetic survey in 1978 (Hildenbrand *et al.* 1993), the anomaly of the total intensity does not exceed 1 μT in Hawaii Island.

(2) The magnetic north direction at our sampling site is consistent with that expected from the IGRF 1995 ($D = 10.1°$), since the difference between the orientation data by both sun and magnetic compasses is $-1.9° \pm 2.2°$ ($N = 18$). Assuming that the standard deviation of 2.2° is produced solely by randomly oriented magnetization vectors with constant length, its magnitude is calculated to be 1.4 μT, not causing approximately 55 per cent stronger palaeointensities.

(3) If the ambient magnetic field were disturbed by the local anomaly, intense NRMs would be acquired at the region with a strong field while small ones at a weak field. In this case the palaeointensities should result in proportion to these NRMs, but there is no correlation between the NRM intensities and the palaeointensities (Table 1).

MD components

It is known that the existence of MD components evokes a concave-up curve in an NRM–TRM plot resulting in an apparent high palaeointensity (Levi 1977; Xu & Dunlop 1995). However, the MD contribution for NRM of our samples are estimated to be less than 13 per cent (Section 3) and this amount does not seem to explain the present anomalous palaeointensities which are as high as 50 per cent. In Levi's (1977) study, one of his samples showed a 6–18 per cent decrease in simulated NRM by the LTD treatment only resulted in a 5 per cent higher palaeointensity for the least-squares fit of its NRM–TRM diagram. He also examined another two samples with a greater MD contribution, namely a 41–53 per cent NRM decrease by the LTD, but they showed 14–21 per cent high palaeointensities at most.

For more careful inspection, we applied the Thellier method combined with the LTD treatment to some sister specimens (A-4-4L, B-9-4L and C-4-4L). This is because the linearity of Arai diagrams would be improved by the treatment and give appropriate palaeointensities if the MD components seriously affected the present results. In the experiment, the samples are chilled in liquid nitrogen for 10 min after each progressive zero-field and in-field heating. These cycles are the same as those in the LTD–DHT Shaw method (Section 4.2). Then the remanence is measured for each step. Arai diagrams are therefore constructed for both LT-survived NRMs and LT-survived laboratory-produced TRMs. They are shown in Figs 5(d)–(f) together with those from the normal Thellier method for the sister specimens. The intensity decrease of these samples by LTD is 8–12 per cent in NRMs.

In contrast to expectations, the LTD treatment exhibited a kind of concave-up feature for groups A and B (Figs 5d and e). Although these concave-up diagrams may not be accepted as successful results in terms of the modern palaeointensity study, it should be noted that there are no reason to reject their lower blocking temperature portion that passes the pTRM test. This is because the MD components capable of apparently high palaeointensities are considered to be removed by the LTD. If we apply the selection criteria (Section 4.1), their linear best-fitting lines gave much higher palaeointensities, above 80 μT. On the other hand, the good linearity of group C in the NRM–TRM plot is preserved as in Fig. 5(f). Resultant palaeointensities with and without the treatment (36.9 and 37.5 μT) are almost the same. These results indicate that the MD effect is not the main reason and that there should be other reasons that can explain these contradictory results. The Day plot (Fig. 2g) also supports this conclusion since the largest contribution of MD components appears in group C while less MD content is expected for groups A and B.

PSD components

Kosterov & Prévot (1998) studied non-ideal behaviour of the Thellier experiments characterized by a rapid decay of NRM without

a relative acquisition of pTRM at moderately low temperatures. They suggested that this behaviour was a result of the transformation of the micromagnetic structure of PSD grains from a metastable configuration to a more stable one. An irreversible decrease in coercivity at relatively low temperature (up to 200–250 °C) would cause such a phenomenon accompanied with an apparently anomalous palaeointensity in the Thellier method. This PSD effect may cause the higher palaeointensities in this study as all the samples are plotted in the PSD region of the Day plot (Fig. 2g). However, the erroneously high palaeointensities in the Thellier method are yielded especially from group B and it is difficult to think that the transformation of PSD works selectively in this group. The two high palaeointensities from B-4-2 and C-2-2 by the LTD–DHT Shaw method also do not seem to support the PSD effect, since this method does not include the stepwise laboratory heating. Therefore, the effect of PSD components cannot be the main reason for the high palaeointensities.

TCRM production in the laboratory

Some studies suggested that TCRM production during laboratory heating could be a cause for erroneous palaeointensities (e.g. Hoffman *et al.* 1989). However, in our study, the pTRM test was positive up to 500–580 °C for nine out of 10 specimens of group B and these Zijderveld diagrams did not show signs of heavy laboratory alteration (e.g. Fig. 5b). Thus, it would be safe to say that laboratory TCRM production is not the main reason for the erroneous intensities.

TCRM production in initial cooling

The most striking feature of the present results is that group C with the highest oxidation indices yields an appropriate palaeointensity, whilst all the palaeointensities from group B with intermediate oxidation are systematically high. It suggests that the oxidation state is related to the erroneous palaeointensities. In fact, Rolph (1992) applied his version of the Shaw method (Shaw 1974; Rolph & Shaw 1985) to Mount Etna lavas, finding a correlation between the high palaeointensities and the high oxidation state. For the Hawaiian 1960 lava, as stated in the several previous studies (Mankinen & Champion 1993; Tsunakawa & Shaw 1994), there is a possibility that it acquired TCRM during its initial cooling stage.

In the present study, we found pseudobrookites from group C specimens. Since the pseudobrookite cannot be formed below 585 °C (e.g. Dunlop & Özdemir 1997, p. 409), it guarantees that equilibrium is achieved above the Curie temperature of the magnetite. Therefore, true TRMs are expected to consist of NRMs for group C and this may be a reason why group C gives an appropriate palaeointensity.

On the other hand, a number of small domains of titanium-poor titanomagnetite surrounded by ilmenite lamellae are observed in group B. It suggests that continuous oxidation occurs below the Curie temperature in the initial cooling stage of the lava.

5.2 Detection of TCRM

It is important to distinguish TCRM from TRM to avoid incorrect palaeointensities. Although its detection seems quite difficult, there are some possible ways. McClelland (1996) suggested that grain growth CRM was detectable by non-linear Arai diagrams over certain temperature intervals because of the difference of the blocking temperature spectra between CRM and TRM in an identical set of magnetic grains. McClelland & Briden (1996) also pointed out that a linear Arai diagram for an original TRM would not be preserved if some amount of CRM is involved.

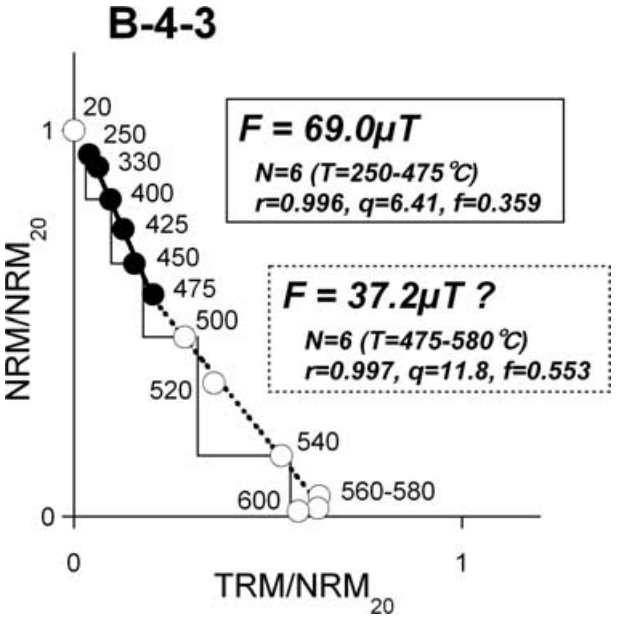

Figure 9. Experimental result of the specimen B-4-3 by the Thellier method. High blocking temperatures of 250–475 °C can yield another linear segment that gives a palaeointensity of 37.2 μT ($r = 0.997$, $q = 11.8$ and $f = 0.553$).

We found such a behaviour only in the experimental result of B-4-3 (Fig. 9). This specimen passed the pTRM test almost throughout the heating temperatures and gave a high palaeointensity of 69.0 μT for the 250–475 °C range (Table 1). However, another linear segment can be seen for the high blocking temperatures of 475–580 °C. It yields a palaeointensity of 37.2 μT ($r = 0.997$, $q = 11.8$ and $f = 0.553$) in agreement with the expected intensity. This suggests that the lower blocking temperature portion is affected by TCRM while the higher one may be composed of TRM. A similar behaviour for two segments was also observed by Hill & Shaw (2000). In their study, almost all the samples from one vertical section of the 1960 lava exhibited two-slope Arai diagrams. Their first segments gave palaeointensities of between 36.0 and 68.7 μT.

The Thellier method with the LTD treatment seems to detect this kind of two-slope behaviour owing to TCRM more clearly. In the results of groups A and B (Figs 5d and e), the low blocking temperature segments yielded very high palaeointensities of 85.5 μT (A-4-4L) and 81.6 μT (B-9-4L). This is probably because the grain growths would more easily produce SD than MD and that these SD components detectable as a LT memory carry TCRM, if the high-temperature oxidation continued below the Curie temperature of the magnetite. On the other hand, for the pseudobrookite-bearing sample in group C (C-4-4L, Fig. 5f), the LTD treatment reveals that no significant TCRM is carried by the LT memory. These ideas can explain the contradictory results in the LTD Thellier experiments (Section 5.1, Figs 5d–f). Therefore, the Thellier method combined with the LTD can be regarded as one of the tools for TCRM detection.

The LTD–DHT Shaw method also seems to be one of the useful tools for TCRM detection. In this method, a number of anomalous results are rejected, especially for group B when compared with the Thellier results (Fig. 10). The reasons for these rejections come from

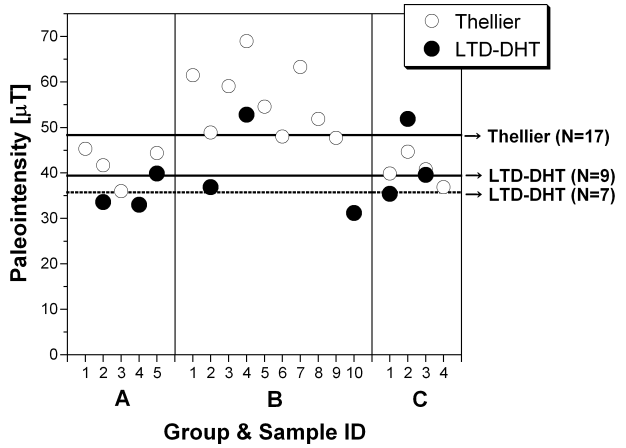

Figure 10. All the palaeointensities measured by the Thellier and LTD–DHT Shaw methods. Vertical and horizontal axes indicate the calculated palaeointensity and the sample ID number, respectively. The results by the Thellier method are shown as open symbols while those by the LTD–DHT Shaw method are shown as closed symbols. The averaged palaeointensities are also shown by solid lines, and an alternative average of the LTD–DHT Shaw method is shown by a dashed line if two outliers of B-4-2 and C-2-2 are excluded. The expected field intensity is 36.2 μT from DGRF 1965.

the double-heating test, the ARM correction and the LTD treatment. Since a CRM/TRM ratio is not wholly constant throughout the grain size for the grain growth CRM (McClelland 1996), a TCRM/TRM ratio is considered to be variable with grain size, that is, coercivity. If NRM is shared by both TRM and TCRM while TRM1 is of a true TRM, the NRM–TRM1* diagram does not necessarily show a linearity. If TCRM is further gained in the laboratory heating, its effect is probably different between TRM1 in the first heating and TRM2 in the second. In this case, the TRM1–TRM2* diagram does not have a unit slope. The LTD treatment may more clearly expose these TCRM effects by removing MD components, similarly to the Thellier experiments. Although two anomalous results of B-4-2 and C-2-2 still survived after applying the selection criteria (Fig. 10), these are statistically more distinguishable than in the Thellier method. As a result, the multispecimen test seems to work better for the TCRM-affected samples in the LTD–DHT Shaw method.

6 CONCLUSIONS

We performed systematic palaeointensity measurements on the Hawaiian 1960 lava. Based on the various rock magnetic analyses, 19 cores used in this study are classified into three groups of A–C. Deuteric oxidation progressed in this order. Coe's version of the Thellier method (Coe 1967) gave an average intensity of 49.0 ± 9.6 μT ($N = 17$), approximately 35 per cent higher than the expected field intensity (36.2 μT). These high palaeointensities are observed mostly from group B, which shows the medium high-temperature oxidation indices of II–IV, and the multispecimen test does not work well. On the other hand, the LTD–DHT Shaw method (Tsunakawa *et al.* 1997; Tsunakawa & Yamamoto 1999) resulted in a better mean of 39.4 ± 7.9 μT ($N = 9$) since most results from group B were rejected by the selection criteria. If two outliers are further excluded, the average is improved to be 35.7 ± 3.3 μT ($N = 7$) in good agreement with the expected value.

As several reasons for the high palaeointensities are examined, the TCRM acquisition during the initial cooling is likely to cause the anomalous results. Although it is difficult to distinguish TCRM from TRM, we can detect its effect by the LTD treatment combined with the Thellier experiment. Another possible tool for TCRM detection is the LTD–DHT Shaw method. Although a few erroneously high palaeointensities are still observed in the results, they are easily judged to be outliers by the multispecimen test. Therefore, the LTD–DHT Shaw method combined with the multispecimen test will be one of the useful tools for obtaining accurate palaeointensity from volcanic rocks. It is also concluded that the palaeointensity determination of volcanic rocks should be made for samples with various oxidation states to discriminate erroneously high intensities arising from TCRM.

ACKNOWLEDGMENTS

We thank Dr Hidefumi Tanaka, Kochi University, for the courtesy of preparing the geographical maps in the sampling. We also appreciate constructive comments by two anonymous reviewers. This study is supported by the 'Super Plume' project of the Science and Technology Agency of Japan.

REFERENCES

Baag, C., Helsley, C.E., Xu, S. & Lienert, B.R., 1995. Deflection of paleomagnetic directions due to magnetization of the underlying terrain, *J. geophys. Res.,* **100,** 10 013–10 027.

Calvo, M., Prévot, M., Perrin, M. & Riisager, J., 2002. Investigating the reason for the failure of paleointensity experiments: a study on historical lava flows from Mt Etna (Italy), *Geophys. J. Int.,* **149,** 44–63.

Coe, R.S., 1967. Paleointensities of the Earth's magnetic field determined from Tertiary and Quaternary rocks, *J. geophys. Res.,* **72,** 3247–3262.

Coe, R.S. & Gromme, S., 1973. A comparison of three methods of determining geomagnetic paleointensities, *J. Geomag. Geoelectr.,* **25,** 415–435.

Coe, R.S., Gromme, S. & Mankinen, E.A., 1978. Geomagnetic paleointensities from radiocarbon-dated lava flows on Hawaii and the question of the pacific nondipole low, *J. geophys. Res.,* **83,** 1740–1756.

Day, R., Fuller, M. & Schmidt, V.A., 1977. Hysteresis properties of titanomagnetites: grain-size and compositional dependence, *Phys. Earth Planet. Int.,* **13,** 260–267.

Dunlop, D.J. & Özdemir, Ö., 1997. *Rock Magnetism: Fundamentals and Frontiers,* Cambridge University Press, Cambridge, p. 573.

Heider, F., Dunlop, D.J. & Soffel, H.C., 1992. Low-temperature and alternating field demagnetization of saturation remanence and thermoremanence in magnetite grains (0.037 μm to 5 mm), *J. geophys. Res.,* **97,** 9371–9381.

Hildenbrand, T.G., Rosenbaum, J.G. & Kauahikaua, J.P., 1993. Aeromagnetic study of the island of Hawaii, *J. geophys. Res.,* **98,** 4099–4119.

Hill, M.J. & Shaw, J., 2000. Magnetic field intensity study of the 1960 Kilauea lava flow, Hawaii, using the microwave paleointensity technique, *Geophys. J. Int.,* **142,** 487–504.

Hoffman, K.A., Constantine, V.L. & Morse, D.L., 1989. Determination of absolute palaeointensity using a multi-specimen procedure, *Nature,* **6222,** 295–297.

Juarez, M.T. & Tauxe, L., 2000. The intensity of the time-averaged geomagnetic field: the last 5 Myr, *Earth planet. Sci. Lett.,* **175,** 169–180.

Kellogg, K., Larson, E.E. & Watson, D.E., 1970. Thermochemical remanent magnetization and thermal remanent magnetization: comparison in a basalt, *Science,* **170,** 628–630.

Kono, M., 1978. Reliability of paleointensity methods using alternating field demagnetization and anhysteretic remanence, *Geophys. J. R. astr. Soc.,* **54,** 241–261.

Kono, M., 1987. Changes in TRM and ARM in a basalt due to laboratory heating, *Phys. Earth planet. Inter.,* **46,** 1–8.

Kono, M., Hamano, Y., Nishitani, T. & Tosha, T., 1984. A new spinner magnetometer: principles and techniques, *Geophys. J. R. astr. Soc.,* **67,** 217–227.

Kono, M., Kitagawa, H. & Tanaka, H., 1997. Use of automatic spinner magnetometer-AF demagnetizer system for magnetostratigraphy and paleosecular variation studies (abstract), *8th Scientifiic Assembly IAGA, Uppsala*.

Kosterov, A.A. & Prévot, M., 1998. Possible mechanisms causing failure of Thellier paleointensity experiments in some basalts, *Geophys. J. Int.,* **134,** 554–572.

Laj, C., Kissel, C., Scao, V., Beer, J., Thomas, D.M., Guillou, H., Muscheler, R. & Wagner, G., 2002. Geomagnetic intensity and inclination variations at Hawaii for the past 98 kyr from core SOH-4 (Big Island): a new study and a comparison with existing contemporary data, *Phys. Earth planet. Inter.,* **129,** 205–243.

Levi, S., 1977. The effect of magnetite particle size on paleointensity determinations of the geomagnetic field, *Phys. Earth planet. Inter.,* **13,** 245–259.

Mankinen, E.A. & Champion, D.E., 1993. Broad trends in geomagnetic paleointensity on Hawaii during holocene time, *J. geophys. Res.,* **98,** 7959–7976.

McClelland, E., 1996. Theory of CRM acquired by grain growth & its implications for TRM discrimination and paleointensity determination in igneous rocks, *Geophys. J. Int.,* **126,** 271–280.

McClelland, E. & Briden, J.C., 1996. An improved methodology for Thellier-type paleointensity determination in igneous rocks and its usefulness for verifying primary tnermoremanence, *J. geophys. Res.,* **101,** 21 995–22 013.

Ozima, M., Ozima, M. & Akimoto, S., 1964. Low temperature characteristics of remanent magnetization of magnetite—self-reversal and recovery phenomena of remanent magnetization, *J. Geomag. Geoelectr.,* **16,** 165–177.

Rolph, T.C., 1992. High field intensity results from recent and historic lavas, *Phys. Earth planet. Inter.,* **70,** 224–230.

Rolph, T.C. & Shaw, J., 1985. A new method of paleofield magnitude correction for thermally altered samples and its application to Lower Carboniferous lavas, *Geophys. J. R. astr. Soc.,* **80,** 773–781.

Roperch, P., Bonhommet, N. & Levi, S., 1988. Paleointensity of the Earth's magnetic field during the Laschamp excursion and its geomagnetic implications, *Earth planet. Sci. Lett.,* **88,** 209–219.

Selkin, P.A. & Tauxe, L., 2000. Long-term variations in paleointensity, *Phil. Trans. R. Soc. Lond.,* A., **358,** 1065–1088.

Shaw, J., 1974. A new method of determining the magnitude of the paleomagnetic field. Application to five historic lavas and five archaeological samples, *Geophys. J. R. astr. Soc.,* **76,** 637–651.

Tanaka, H., 1999. Theoretical background of ARM correction in the Shaw paleointensity method, *Geophys. J. Int.,* **137,** 261–265.

Tanaka, H. & Kono, M., 1991. Preliminary results and reliability of paleointensity studies on historical and ^{14}C dated Hawaiian lavas, *J. Geomag. Geoelectr.,* **43,** 375–388.

Tanaka, H., Kono, M. & Kaneko, S., 1995. Paleosecular variation of direction and intensity from two Pliocene–Pleistocene lava sections in southwestern Iceland, *J. Geomag. Geoelectr.,* **47,** 89–102.

Tanaka, H., Kawamura, K., Nagao, K. & Houghton, B.F., 1997. K-Ar ages and paleosecular variation of direction and intensity from Quaternary lava sequence in the Ruapehu volcano, New Zealand, *J. Geomag. Geoelectr.,* **49,** 587–599.

Tarduno, J.A., Cottrell, R.D. & Smirnov, A.V., 2001. High geomagnetic intensity during the Mid-Cretaceous from Thellier analyses of single plagioclase crystals, *Science,* **291,** 1779–1783.

Thellier, E. & Thellier, O., 1959. Sur l'intensite du champ magnetique terrestre dans le passe historique et geologique, *Ann. Geophys.,* **15,** 285–376.

Tsunakawa, H. & Shaw, J., 1994. The Shaw method of paleointensity determinations and its application to recent volcanic rocks, *Geophys. J. Int.,* **118,** 781–787.

Tsunakawa, H. & Yamamoto, Y., 1999. Paleointensity measurement of the Hawaiian 1960 lava and its implications for the reliability of paleointensity determinations (abstract), *EOS, Trans. Am. geophys. Un.,* **80,** Fall Meeting suppl., F300–301.

Tsunakawa, H., Shimura, K. & Yamamoto, Y., 1997. Application of double heating technique of the Shaw method to the Brunhes epoch volcanic rocks (abstract), *8th Scientific Assembly IAGA, Uppsala*.

Valet, J.P. & Herrero-Bervera, E., 2000. Paleointensity experiments using alternating field demagnetization, *Earth Planet. Sci. Let.,* **177,** 43–58.

Vlag, P., Alva-Valdivia, L., de Boer, C.B., Gonzalez, S. & Urrutia-Fucugauchi, J., 2000. A rock- and paleomagnetic study of a Holocene lava flow in Central Mexico, *Phys. Earth planet. Inter.,* **118,** 259–272.

Watkins, N.D. & Haggerty, S.E., 1967. Primary oxidation variation and petrogenesis in a single lava, *Contr. Mineral. and Petrol.,* **15,** 251–271.

Wilson, R.L. & Watkins, N.D., 1967. Correlation of petrology and natural magnetic polarity in Columbia Plateau basalts, *Geophys. J. R. astr. Soc.*, **12,** 405–424.

Xu, S. & Dunlop, D.J., 1995. Thellier paleointensity determination using PSD and MD grains (abstract), *EOS, Trans. Am. geophys. Un.,* **76,** Fall Meeting suppl., F170.